Noname manuscript No.
(will be inserted by the editor)

Forest Stand Height Estimation using Inversion of RVoG Model over Forest of North-Eastern India

Ankita Mungalpara · Sanid Chirakkal · Deepak Putrevu

Received: date / Accepted: date

Abstract Multiple studies have been carried in recent years to estimate forest height using remote sensing techniques. The forest height is an essential forest resource parameter that is usually used in biomass estimation contributing to carbon sequestration studies. Polarimetric Interferometric SAR (PolInSAR) is a remote sensing technique that combines SAR Polarimetry (PolSAR) with SAR Interferometry (InSAR) and has demonstrated tremendous ability for forest height extraction as it is sensitive to the vertical arrangement of the scattering media. In this paper, we examine the Random Volume over Ground (RVoG), the polarimetric canopy scattering model, for the forward modeling, and the three-stage inversion (TSI) for retrieving vegetation stand height. We investigate the performance of the inversion algorithm for forest height estimation using single baseline L-band ALOS-2 PALSAR data collected on December 17, 2018, and December 31, 2018, over the Saipung Reserve Forest, Meghalaya, over North-Eastern India. Correlation between the field measured forest height, and the estimated tree height using the TSI technique is 0.81 with RMSE of 5.05 m. The study suggests that the PolInSAR approach has significant potential for retrieval of forest biophysical parameters such as stand height.

Keywords . Synthetic Aperture Radar (SAR) · Forest Height Estimation · Polarimetric Interferometric SAR (PolInSAR)

Ankita Mungalpara
DA-IICT, Gandhinagar, Gujarat 382007, India
E-mail: mungalpara.ankita@gmail.com

Sanid Chirakkal
SAC, ISRO, Ahmedabad, Gujarat, 380015, India
E-mail: sanid@sac.isro.gov.in

Deepak Putrevu
SAC, ISRO, Ahmedabad, Gujarat, 380015, India
E-mail: dputrevu@sac.isro.gov.in

1 Introduction

The prime carbon sinks are the temporal biosphere (soil, vegetation) and oceans where atmospheric carbon sequesters. Changing carbon content in the atmosphere gradually affects the carbon cycle and climate due to the greenhouse effect. Assessing the forest biomass is vital for monitoring the quantity of carbon that is impacted by deforestation and the estimation of carbon stock in a forest ecosystem [1]. Forest height is an unusual parameter to consider for assessment of the carbon reserve. Information about forest height is essential to carbon stock evaluation and classification of vegetation types. It is also crucial to determine the weather influence, diseases in vegetation, and unlawful cutting of trees. It has been reported that deforestation practices have vastly contributed to global climate change [2]. Because of these reasons, accurate tracking and measures to achieve a better understanding of the Earth's carbon cycle are very important for sustaining life [3]. These inferences make research on retrieval of forest height information quite essential.

Vegetation parameter estimation (using remote sensing techniques), at large scale, is very critical to perform ecosystem modeling effectively and to address essential science questions related to climate change, global warming, etc. [4]. The interferometric technique of SAR-based sensing has shown great potential to retrieve forest height with reliable accuracy [5]. In the last years, quantitative model based estimation of forest parameters based on single frequency fully polarimetric single-baseline configuration has been developed and demonstrated over a variety of test sites [6] [7] [8]. Polarimetric SAR Interferometry (PolInSAR), together with an appropriate inversion model such as the Random Volume over Ground (RVoG) [9] [10] [11], has demonstrated a significant success for the recovery of canopy height and of the underlying ground elevation. RVoG is a polarimetric canopy scattering model describing the vertical structure of the forest as two layers, namely, the ground and the canopy [12].

In this paper, we showcase an algorithm based on single-baseline PolInSAR to retrieve one of the vital vegetation parameters, viz., the canopy height. PolInSAR combines the utilities of two SAR technologies: Polarimetry and Interferometry. PolSAR (Fully Polarimetric Synthetic Aperture Radar) provides the three complex scattering matrices at each image pixel, which provides insight into the structural information of the scatterer (geometry, shape, and dielectric constant). InSAR (Interferometric SAR) leads to interferogram generated out of SAR images acquired with an appropriate baseline (spatial or temporal). A common problem for all estimation techniques emerges from the nature of the scattering process. In terms of the interferometric observables, it does not provide an effective separability of the physical forest parameters. This limits a straightforward parameter estimation and requires the inversion of a scattering model, which relates the interferometric observables to the physical parameters of the scattering process [9] [13]. This is where combining PolSAR with InSAR becomes advantageous. In this paper, we examine the RVoG, the polarimetric canopy scattering model, for the forward model-

ing, and the three-stage inversion (TSI) for retrieving vegetation stand height. This inversion also estimates other forest parameters such as canopy extinction, ground-to-volume amplitude, and ground topographic phase [10].

2 Methodology

This research majorly focuses on the estimation of forest height using PolInSAR data collected by L-band spaceborne sensor while taking into consideration the impact of changing the extinction coefficient on the estimation precision. The following methodology is adopted to achieve the aim of this research:

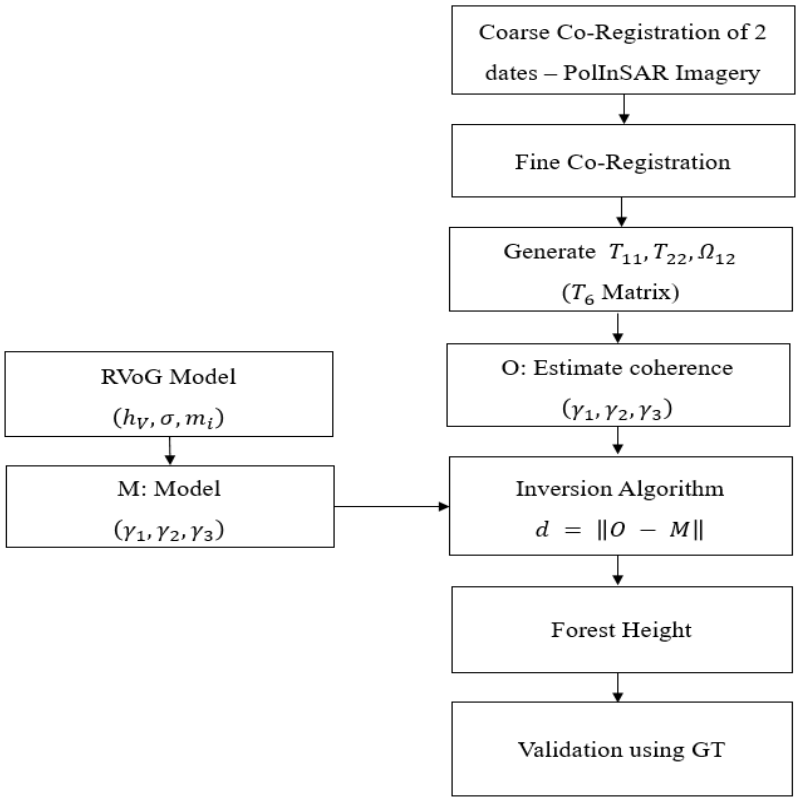

Fig. 1: Methodology for PolInSAR processing

2.1 PolInSAR Data Processing

The PolInSAR data processing takes into account two acquisitions of the same area from different times on December 17, 2018, and December 31, 2018. For this study, ALOS-2 PALSAR acquisition with a single spatial baseline is used. Absolute radiometric calibration considers both the backscatter and the radar brightness and minimizes the difference between the radiometry of acquisitions done on differential geometry. The data is calibrated for pixel values to represent the true backscatter. The complex outputs after calibration are stored to acquire useful information of both phase and amplitude for forest height estimation.

2.1.1 Generation of Scattering Matrix

The scattering matrix stores the values from the different polarization channels. The scattering matrix for all the datasets is formed to obtain the backscatter information. The 2×2 matrices of the dataset are used for analysis as a pair of master and slave with scattering matrix $[s_1]$ and $[s_2]$, respectively in the horizontal-vertical basis as:

$$[S_1] = \begin{bmatrix} S^1_{HH} & S^1_{HV} \\ S^1_{VH} & S^1_{VV} \end{bmatrix} \tag{1}$$

$$[S_2] = \begin{bmatrix} S^2_{HH} & S^2_{HV} \\ S^2_{VH} & S^2_{VV} \end{bmatrix} \tag{2}$$

Where 1 and 2 represent the superscripts.

2.1.2 Co-registration

Co-registration aligns images to provide backscatter information from the same ground position while minimizing the loss in coherence. Vertical wavenumber correlates the phase information to the height of the scatterer and is calculated using the Equation (3). For a positive slant, the value of κ_z is more than for a negative slant. The height estimation uses κ_z a scaling factor. SAR geometry computation is used to obtain a suitable range of κ_z.

$$\kappa_z = \frac{\kappa \Delta\theta}{\sin\theta_0} \quad \kappa = \frac{4\pi}{\lambda} \tag{3}$$

Where θ_0 is the angle of incidence, $\Delta\theta$ is the apparent angular separation of the baseline B from scattering point, and λ is the wavelength for L-band Interferometric system.

2.1.3 Coherency and Covariance Matrix Generation

To collect scattering information from multiple targets within a pixel (also, distributed scatterer) coherency matrix $[T_6]$ and covariance matrix are generated. The information from only the scattering matrix is inadequate to explain the backscatter from multiple scatterers.

A monostatic, fully polarimetric interferometric system maps each resolution element in the view from two slightly different look angles, two scattering matrices $[s_1]$, and $[s_2]$. Assuming reciprocal scattering, the 3-D Pauli-scattering vectors $\mathbf{k}_1$ and $\mathbf{k}_2$ are then given by [15],

$$\mathbf{k}_1 = \frac{1}{\sqrt{2}} \left[S^1_{HH} + S^1_{VV}, S^1_{HH} - S^1_{VV}, 2S^1_{HV} \right]^T \tag{4}$$

$$\mathbf{k}_2 = \frac{1}{\sqrt{2}} \left[S^2_{HH} + S^2_{VV}, S^2_{HH} - S^2_{VV}, 2S^2_{HV} \right]^T \tag{5}$$

Where 1 and 2 represent the superscripts. Then a six-dimension complex matrix $[T_6]$ of PolInSAR can be represented as [13],

$$[T_6] = \left\langle \begin{bmatrix} \mathbf{k}_1 \\ \mathbf{k}_2 \end{bmatrix} \begin{bmatrix} \mathbf{k}_1^{*T} & \mathbf{k}_2^{*T} \end{bmatrix} \right\rangle = \begin{bmatrix} T_{11} & \Omega_{12} \\ \Omega_{12}^{*T} & T_{22} \end{bmatrix} \tag{6}$$

The complete information estimated by the SAR system can be represented in the form of three 3×3 complex matrices $[T_{11}]$, $[T_{22}]$, and $[\Omega_{12}]$ formed using the outer products of $\mathbf{k}_1$ and $\mathbf{k}_2$.

2.1.4 Coherence Estimation

The complex coherence is formed after vectorization of the interferometric coherence, and the general vector expression for coherence is as expressed [13],

$$\tilde{\gamma} = \frac{\left\langle \overrightarrow{\omega_1}^{\dagger} \left[\Omega_{12} \right] \boldsymbol{\omega}_2 \right\rangle}{\sqrt{\left\langle \boldsymbol{\omega}_1^{\dagger} \left[T_{11} \right] \boldsymbol{\omega}_1 \right\rangle \cdot \left\langle \overrightarrow{\omega}_2^{\dagger} \left[T_{22} \right] \boldsymbol{\omega}_2 \right\rangle}} \tag{7}$$

Where $\langle ... \rangle$ represents the expected value applied for averaging and $\dagger$ denotes the complex conjugate transpose, $[\Omega_{12}]$, $[T_{11}]$ and $[T_{22}]$ are the coherence matrices calculated from the polarimetric scattering vectors $\mathbf{k}_1$ and $\mathbf{k}_2$ associated to the images of the interferometric pair.

$$\tilde{\gamma}\left(\boldsymbol{\omega}_1, \boldsymbol{\omega}_2\right) = \frac{\boldsymbol{\omega}^{*T} \Omega \boldsymbol{\omega}}{\boldsymbol{\omega}^{*T} T \boldsymbol{\omega}} \tag{8}$$

It can be rewritten as Equation (8) when $T = \left(T_{11} + T_{22}\right)/2$ and $\boldsymbol{\omega}_1 = \boldsymbol{\omega}_2 = \boldsymbol{\omega}$ with $0 \leq |\tilde{\gamma}| \leq 1$.

2.1.5 Random Volume over Ground (RVoG) Scattering Model

In the forest observation, both ground and canopy back-scattering is carried in the received signals. For the extraction of physical parameters from interferometric data, a coherent model of the scattering process which relates the measurables to the desired parameters is required [11] [14]. A realistic scattering model has to consider both the vegetation layer and ground interactions in the case of forest scattering at L-band. A most simple model to describe such a scenario is the Random Volume over Ground (RVoG) scattering model. This model considers the ground scatter for the inversion process.

Thus, the vegetation layer is defined as a thickness layer, carrying a volume of randomly oriented particles and scattering amplitude per unit volume m_V. This random volume is located over a ground scatterer positioned at $z = z_0$ with scattering amplitude m_G. Through the vegetation layer, the ground is observed by an interferometric system operating at a wavelength λ with a physical baseline B under a mean incident angle θ_0 at the range R. In this instance, the complex interferometric coherence $\tilde{\gamma}$, after range spectral filtering, written as [11] [14],

$$\tilde{\gamma}(\omega) = e^{i\phi_0} \frac{\tilde{\gamma}_V + m(\boldsymbol{\omega})}{1 + m(\boldsymbol{\omega})} = e^{i\phi_0} \left(\tilde{\gamma}_V + \frac{m(\boldsymbol{\omega})}{1 + m(\boldsymbol{\omega})} (1 - \tilde{\gamma}_V) \right) \tag{9}$$

Equation (9) can also be written as:

$$\tilde{\gamma}(\omega) = e^{i\phi_0} \left(\tilde{\gamma}_V + F(\omega) (1 - \tilde{\gamma}_V) \right) \tag{10}$$

Where $\boldsymbol{\omega}$ is a unitary vector that describes the polarization, $\tilde{\gamma}_V$ is the volume coherence, θ_0 is the phase related to the ground topography and m is the effective ground to volume scattering ratio accounting for the attenuation through the volume represented as,

$$m(\overrightarrow{w}) = \frac{m_G(\overrightarrow{w})}{m_V(\overrightarrow{w})} \exp\left(-\frac{2\sigma h_V}{\cos\theta_0} \right) \tag{11}$$

$F(\omega)$ lies in the range $0 < F(\omega) < 1$ with m = 0 for pure volume scattering and $m = \infty$ for pure surface scattering. m is the only parameter that changes with the polarization channel. In RVoG model, the coherence and phase are not independent quantities as it assumes an exponential structure-function in the volume.

2.2 PolInSAR Model Inversion

Inversion of Equation (9) is greatly facilitated by applying a geometrical representation inside the unit circle of the complex coherence plane.

Figure 2 on the next page shows how the model maps coherence points from Equation (9) onto a line in the complex plane. This line has three important features. (1) The line crosses the circle at two localities, i.e., A and B. One of

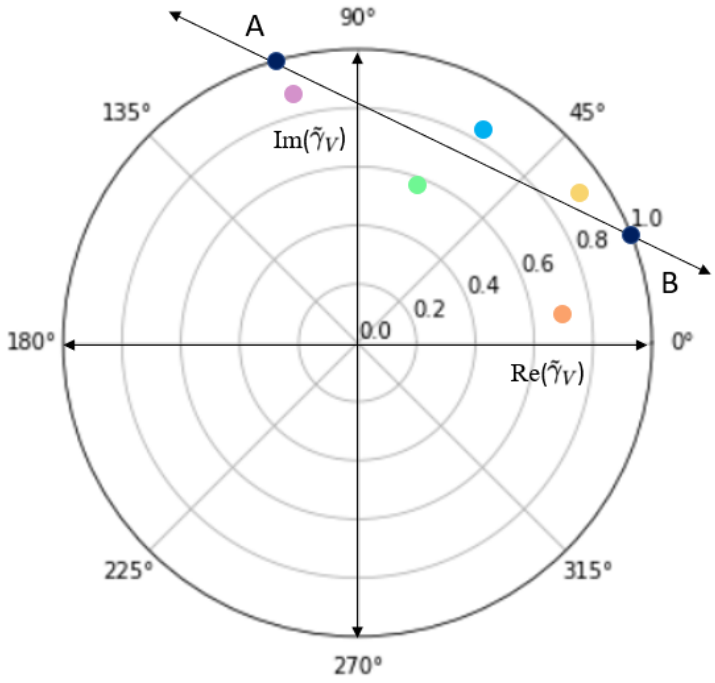

Fig. 2: Line model for polarimetric variation of interferometric coherence

these is the underlying topography related phase. The other solution is a false one and must be rejected through the process of inversion. (2) The volume coherence rests at one end of the line. It is presented as point A in Figure 2. This point is central to height and extinction estimation and therefore, should be estimated from the data. (3) The visible line length in the data can be only a fraction of AB, and neither A nor B can be observed directly.

Inversion of Equation (9) involves taking observations of the complex coherence at several different polarization and then minimizing the difference between the model predictions and observations in the least-squares sense.

2.2.1 Least Square Line Fitting

The first stage is to find the best-fit straight line inside the unit circle of interferometric coherence. One way to get it done is to use a total least squares line fit to the real and imaginary elements of the data and then use the line parameter estimates to secure the intersection points. Alternatively, a faster least-squares line fit in the real and/or imaginary parts can secure an estimate of the minimum error solution.

It can be seen that the complex coherence follows a straight line in the coherence unit circle which intersects the circle at two points. One of the two

points corresponds to the underlying topography phase, so this point is called the true ground phase point; the "pure" volume coherence will be the furthest away in the distance from the true ground phase point along the line.

2.2.2 Vegetation Bias Removal

Through the least square fitting of the observed complex correlations under different polarimetric channels, the ground phase and volume correlation can be extracted from the geometric relationship between the coherent line and unit circle. After that, allowing for the nonlinear property of the coherent volume function, a two-dimensional (2D) search is carried out to accomplish the estimation of forest height and mean extinction. While HH + VV and HH - VV can change relative position depending on whether direct ground or dihedral effects are dominant, it is very unlikely that the most robust ground-to-volume component will arise in the HV channel. It is based on scattering physics, which indicates that dihedral effects in vegetation generally lie orthogonal to HV, direct ground backscatter at L-band has only a weak HV signal.

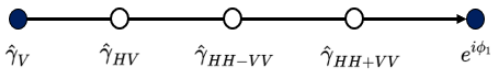

Fig. 3: Relative location of polarization states along the coherence line

Using this procedure, we can now select the appropriate model and generate an interferogram, the phase of which, ϕ, corresponds directly to the true ground topography estimate. Note that this can be achieved through a combination of line fitting and rank ordering of coherence, both of which are fast processes to compute.

2.2.3 Height Estimation

To estimate the two remaining parameters, height, and extinction, we use the estimate of ground phase ϕ, together with the following equation, to find the intersection point among the coherence line and the curve, corresponding to the height/extinction variations:

$$\widetilde{\gamma}_V = \frac{2\sigma}{\cos\theta_o\left(e^{(2\sigma h_V)/\cos\theta_o}-1\right)} \times \int_0^{h_V} e^{ik_z x}\, e^{((2\sigma x)/\cos\theta_o)}\, dx \tag{12}$$

Figure 4 on the next page demonstrates the geometry of this intersection process. The ground phase in this simulation lies at zero degrees, and we show three simulated coherence values along the line. By fixing σ at two different values and then varying the height, we obtain three coherence loci, as shown

in Figure 4. Where the curve intersects the line, we have a candidate $\tilde{\gamma_V}$ point. We show three such intersections. The unambiguous height estimation with single baseline polarimetric interferometry requires that $\tilde{\gamma_V}$, be observed in the data. The robustness of the height inversion process then rests on this assumption. Note, however, that $\tilde{\gamma_V}$ must itself lie on the line, and hence the ambiguous solutions are also constrained to this line.

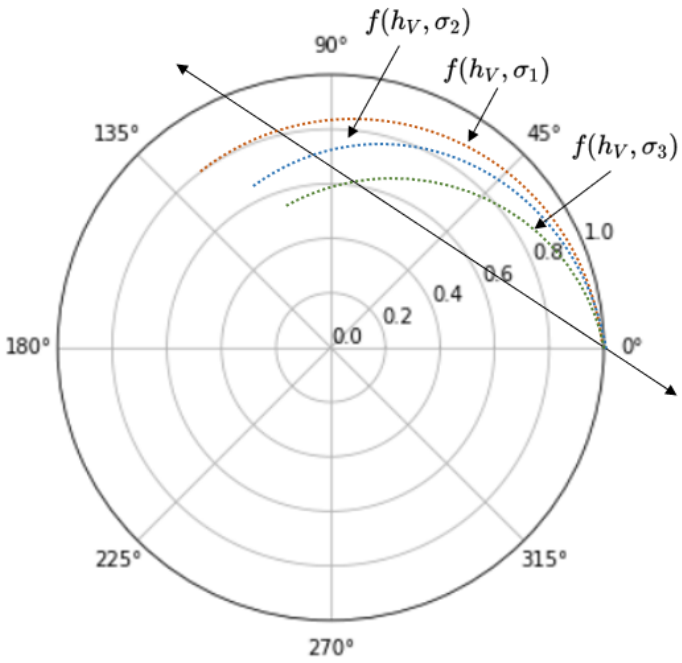

Fig. 4: Geometrical representation of height estimation

3 Study Area and Dataset

3.1 Test Site

The study was conducted in the Saipung Reserve Forest, East Jaintia Hills district of the Jaintia Hills autonomous district council (JHADC) (25°11′24″ E to 25°18′36″ E Latitude and 92°34′30″ N to 92°52′30″ N Longitude) covers 144 km^2, located in Meghalaya, a state situated in the north-eastern corner of India. It is located on the southern slope of the Meghalaya plateau extending from east to west. It is part of the Indomalayan biodiversity hotspot.

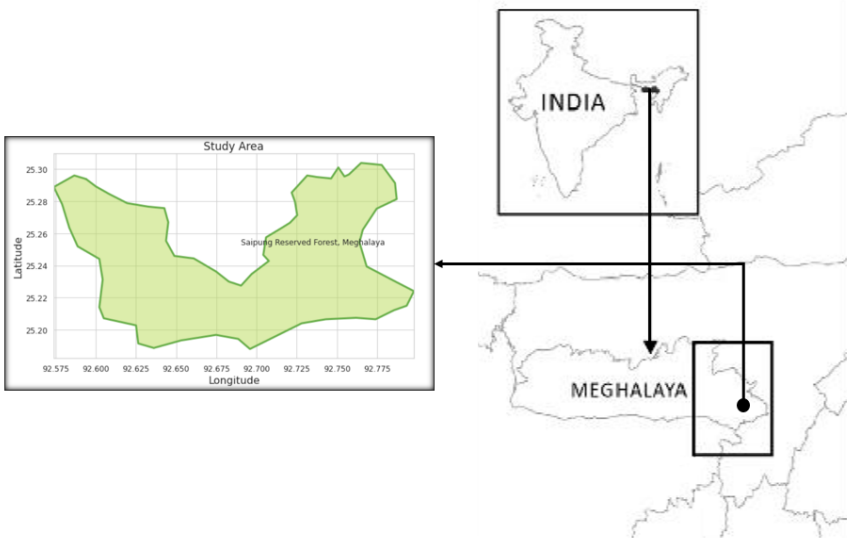

Fig. 5: Location map of Saipung Reserve Forest

3.2 Dataset

For the study, the PolInSAR dataset is used, and for validation purposes, field data are used.

3.2.1 Satellite Data

An interferometric pair of fully polarimetric ALOS-2 PALSAR data has been acquired for Saipung reserve forest to study the effect of inversion of the RVoG model on height retrieval. This dataset was acquired on December 17, 2018, (Master) and December 31, 2018, (Slave). The images were acquired by L-band satellites.

Table 1: Data characteristics of polarimetric interferometric data pair for 2018

Description	Dataset
Date of acquisition	December 17, 2018, and December 31, 2018
Number of Images	2
Band	L
Polarizations	HH, HV, VH, VV

The data is in a Tagged Image File (TIF) format with phase and amplitude information. Since the L-band has a small wavelength, it loses coherence with

a longer time, thus subsiding the quality of interferometric pairs. Therefore, from the datasets available, the pairs with minimum temporal baseline are used for this study. The near-zero temporal baseline ensures that coherence is not reduced due to changes in time of scene acquisition. Small temporal baselines lead to low temporal decorrelation and prevent fluctuations in coherence and phase in interferometric pairs. A detailed description of the dataset used is provided in Table 1.

3.2.2 Field Survey

(a)

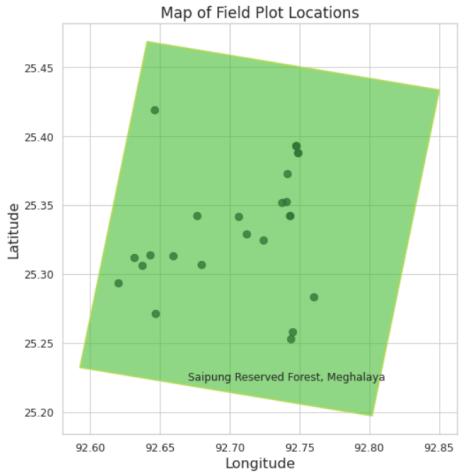

(b)

Fig. 6: (a) Field survey of Saipung Reserve Forest, Meghalaya (b) Field plot locations in Saipung Reserve Forest

A field survey was carried out in December 2018 for the accuracy assessment of the results derived from the SAR data processing. Maps from the Meghalaya Forest Department gave details about the forest types and helped plan the field data collection. The site was selected in such a way that it was possible to see the top and bottom of the tree.

The geo-location was obtained by Trimble Juno SB handheld GPS receiver. The positional error was observed between 7 m - 10 m. Firstly the horizontal distance to the target is calculated then angle to the target base and the top. Once this three-point measurement is achieved, the height of the tree is displayed on the screen. This instrument is accurate up to 0.5 m. The average height of trees in the plots and the latitude and longitude positions were measured. Figure 6b shows the location of points collected in the Saipung Reserve Forest.

3.2.3 Software

- Python 3.6 (Jupyter Notebook, Google Colaboratory) is used for data preprocessing, scattering model implementation, three-stage inversion model, validation, and accuracy assessment.
- ArcGIS developed by ESRI is used for creating coherence height maps.

4 Results and Discussion

The tree height is estimated using the Inversion of RVoG algorithm, and the accuracy assessment for tree height has been done using field data. It includes results from the dataset taken in 2018. It is found that by altering the spatial baseline, the estimation accuracy varied vastly.

4.1 Effect of Ground on The Interferometric Coherence

The figure 7 shows the dependency of the interferometric coherence of the volume layer alone $|\tilde{\gamma}_V|$ on the extinction coefficient σ and the height h_V according to Equation (12) (see Sect. 2.2.3) for the case of an L-band interferometric system ($\lambda = 0.24$ m) with a baseline B (25 m) and incident angle $\theta_0 = 30°$. It demonstrates the height-extinction ambiguity in the interpretation of the interferometric coherence. High vegetation with a high extinction coefficient may be characterized by the same coherence as tall vegetation with a lower extinction coefficient, as both cases may have the same attenuation length. Hence, the interferometric coherence alone is not sufficient for unambiguous extraction of vegetation height from interferometric data.

The influence of ground scattering on the interferometric coherence $|\tilde{\gamma}_V|$ is demonstrated in the Figure 8, where the variation of $|\tilde{\gamma}_V|$ as a function of the ground-to-volume amplitude ratio m and the height h_V for a fixed extinction $\sigma = 0.2$ dB/m, in terms of Equation (9) (see Sect. 2.1.5) is shown.

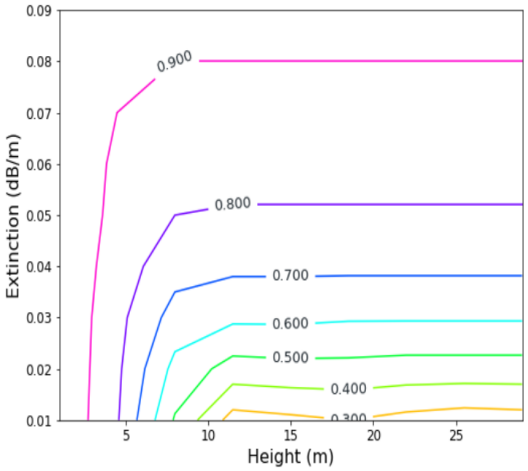

Fig. 7: Interferometric coherence as a function of volume height h_V and extinction coefficient σ (m = 0)

As the ground component increases from zero, the effective phase center moves toward the ground, increasing the effective height distribution of the scatterers and reducing the interferometric coherence.

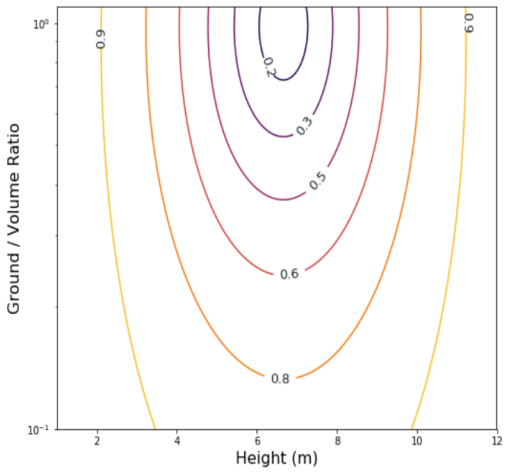

Fig. 8: Interferometric coherence as a function of volume height h_V and ground-to-volume amplitude m (σ = 0.2 dB/m)

4.2 Estimation of Tree Height

The results of TSI are shown in Table 2 for a subset of ground truth points. It shows the estimated height for different field locations in meters collected during the December 2018 expedition to the national reserve forest (carried out through the Principal Chief Conservator of Forests, Meghalaya). It is clear from the table that TSI performs well for our study area with enough sensitivity to the low and high end of the vegetation stand height.

Table 2: Estimated height in meters for study area

Long	Lat	Field Height(m)	Retrieved Height(m)
92.7406	25.3527	24.0	24.8
92.7428	25.3427	27.0	28.9
92.7477	25.3929	4.3	6.4
92.7491	25.3881	6.1	6.4
92.7066	25.3418	14.6	13.9
92.7239	25.3247	21.2	21.0
92.7119	25.3291	24.4	19.5
92.6463	25.4191	20.0	21.1
92.6316	25.3120	11.8	4.8
92.6466	25.2713	8.7	5.7
92.7476	25.3929	4.3	3.8
92.7376	25.3516	1.0	0.4
92.7414	25.3729	1.0	2.4
92.7437	25.2533	17.6	16.1
92.7447	25.2581	20.5	21.6
92.7603	25.2835	18.3	15.1
92.6200	25.2936	12.8	11.9
92.6429	25.3137	25.3	24.8
92.6594	25.2133	17.5	19.0
92.6800	25.3072	26.2	26.5
92.6763	25.3422	19.4	18.5
92.6375	25.3061	21.1	18.9

Figure 9 shows the forest stand height map for Saipung Reserve Forest over the North-Eastern part of India. As can be seen, most of the reserve forest is quite dense with average height shooting above 25 m.

This research's primary purpose is to estimate forest height from the PolInSAR inversion. A regression analysis was carried out to appraise the accuracy of the TSI method. For this, we use the ground truth data of field-measured height, some of which were already shown in Table 2. The correlation coefficient between estimated and field-measured tree height is 0.81 for three-stage inversion. It indicates that the modeled height provides a statistically significant relationship with the field measured height.

The RMSE of the retrieval is found to be approximately 5 meters. This is in agreement with other studies reported in the literature using single-baseline PolInSAR. This figure can be improved by using multi-baseline techniques or using more sophisticated canopy scattering models.

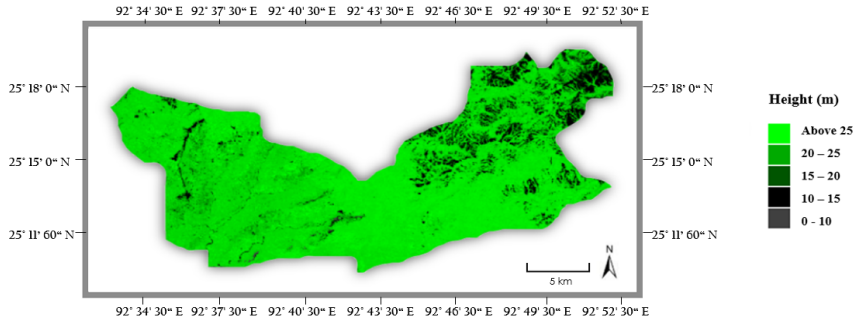

Fig. 9: Saipung Reserve Forest height map derived using the PolInSAR based technique outlined in the paper. It shows the sensitivity of retrieval to the varying height zones of the reserve forest.

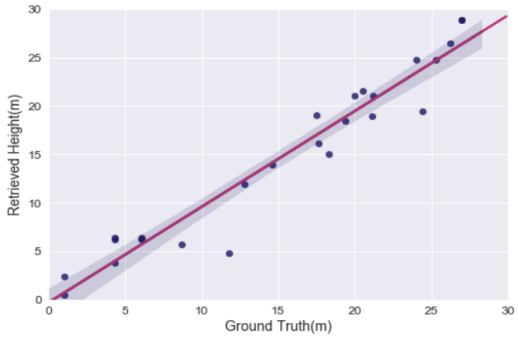

Fig. 10: Retrieved height using Three-stage Inversion (TSI)

5 Conclusion

In this work, PolInSAR forest height estimation is established from the L-band dataset acquired from ALOS-2 PALSAR system. The RVoG canopy scattering model and the three-stage inversion have been implemented (Python 3) to estimate vegetation stand height. This study suggests that the PolInSAR technique has significant potential for retrieving forest biophysical parameters such as stand height, and can substantially augment the biomass estimation over areas like reserve forests where accessibility for field data collection remains difficult.

References

1. Vashum, Kuimi., "Methods to Estimate Above-Ground Biomass and Carbon Stock in Natural Forests - A Review", *Journal of Ecosystem & Ecography*, 02,10.4172/2157-7625.1000116 (2012)

2. Dixon, R.K.K. Solomon, Allen Brown, Sandra Houghton, Richard Trexier, M Wisniewski, J., "Carbon Pools and Flux of Global Forest Ecosystems", *Science (New York, N.Y.)*, 263. 185-90. 10.1126/science.263.5144.185 (1994)
3. Kumar, Shashi Govil, Himanshu Srivastava, Prashant Thakur, Praveen Kushwaha, Satya, "Spaceborne Multifrequency PolInSAR-Based Inversion Modelling for Forest Height Retrieval", *Remote Sensing*, 12, 1-27, 10.3390/rs12244042 (2020)
4. M. Simard, K. Zhang, V. H. Rivera-Monroy, M. Ross, P. Ruiz, E. Castaeda-Moya, E. Twilley, E. Rodriguez, "Mapping Height and Biomass of Mangrove Forests in the Ever glades National Park with SRTM Elevation Data", *Photogrammetric Engineering & Remote Sensing*, vol. 72, No. 3, pp. 299-311 (2006)
5. Balzter, Heiko Rowland, C.S. Saich, P., "Forest canopy height and carbon estimation at Monks Wood National Nature Reserve, UK, using dual-wavelength SAR interferometry", *Remote Sensing of Environment*, 108, 224-239, 10.1016/j.rse.2006.11.014 (2007)
6. Hajnsek, Irena Kugler, F. Lee, Seungkuk Papathanassiou, Kostas, "Tropical Forest Parameter Estimation by means of Pol-InSAR: The INDREX-II Campaign", *IEEE Transactions on Geoscience and Remote Sensing*, 47, 481-493 (2009)
7. Praks, Jaan Kugler, F. Papathanassiou, K. Hallikainen, Martti, "Forest height estimates for boreal forest using L- and X-band polinsar and hutscat scatterometer", *xtEuropean Space Agency, (Special Publication) ESA SP* (2007)
8. Kugler, F. Koudogbo, Fifamè Gutjahr, Karlheinz Papathanassiou, Konstantinos, "Frequency Effects in Pol-InSAR Forest Height Estimation", in *Proc., EUSAR, Dresden, Germany*, 1-4 (2006)
9. Konstantinos P. Papathanassiou and Shane R. Cloude, "Single-Baseline Polarimetric SAR Interferometry", *IEEE Transactions on Geoscience and Remote Sensing*, vol. 39 (2001)
10. S. Cloude and K. Papathanassiou, "Three-stage inversion process for polarimetric SAR interferometry", *Radar, Sonar and Navigation, IEE Proceedings*, vol. 150, pp. 125 – 134 (2003)
11. R. N. Treuhaft and P. R. Siqueira, "Vertical structure of vegetated land surfaces from interferometric and polarimetric radar", in *Radio Science*, vol. 35, no. 1, pp. 141-177, doi: 10.1029/1999RS900108 (2000)
12. C. Wu, C. Wang, P. Shen, J. Zhu, H. Fu and H. Gao, "Forest Height Estimation Using PolInSAR Optimal Normal Matrix Constraint and Cross-Iteration Method", in *tIEEE Geoscience and Remote Sensing Letters*, 16, 8, 1245-1249, 10.1109/LGRS.2019.2895869 (2019)
13. Shane Robert Cloude and Konstantinos P. Papathanassiou, "Polarimetric SAR Interferometry", *IEEE Transaction on Geoscience and Remote Sensing*, vol. 36 (1998)
14. R. N. Treuhaft, S. N. Madsen, M. Moghaddam and J. J. v. Zyl, "Vegetation characteristics and underlying topography from interferometric radar", in *Radio Science*, vol. 31, no. 6, pp. 1449-1485, Nov.-Dec. 1996, doi: 10.1029/96RS01763 (1996)
15. Floyd M Henderson, "Principles and applications of imaging radar", *J. Wiley*, New York (1998)